Asadchy, Viktar S.; "Ra'di", Younes; Vehmas, Joni; Tretyakov, Sergei A.

Functional Metamirrors Using Bianisotropic Elements

P H Y S I C A L   R E V I E W   L E T T E R S

Functional Metamirrors Using Bianisotropic Elements

V. S. Asadchy,[1,2,*] Y. Ra'di,[1] J. Vehmas,[1] and S. A. Tretyakov[1]

[1]*Department of Radio Science and Engineering, Aalto University, P.O. Box 13000, FI-00076 Aalto, Finland*
[2]*Department of General Physics, Francisk Skorina Gomel State University, 246019 Gomel, Belarus*

Conventional mirrors obey the simple reflection law that a plane wave is reflected as a plane wave, at the same angle. To engineer spatial distributions of fields reflected from a mirror, one can either shape the reflector or position some phase-correcting elements on top of a mirror surface. Here we show, both theoretically and experimentally, that full-power reflection with general control over the reflected wave phase is possible with a single-layer array of deeply subwavelength inclusions. These proposed artificial surfaces, metamirrors, provide various functions of shaped or nonuniform reflectors without utilizing any mirror. This can be achieved only if the forward and backward scattering of the inclusions in the array can be engineered independently, and we prove that it is possible using electrically and magnetically polarizable inclusions. The proposed subwavelength inclusions possess desired reflecting properties at the operational frequency band, while at other frequencies the array is practically transparent. The metamirror concept leads to a variety of applications over the entire electromagnetic spectrum, such as optically transparent focusing antennas for satellites, multifrequency reflector antennas for radio astronomy, low-profile conformal antennas for telecommunications, and nanoreflectarray antennas for integrated optics.

Conventional mirrors, known since the dawn of civilization [1], obey the simple law of reflection: the reflection angle is equal to the incidence angle. This follows from the fact that the total tangential electric field at the ideal mirror surface is zero; thus, the phase of the electric field in the reflected wave is the opposite to that in the incident wave. If a reflector can be engineered to enable general control over the reflection phase, it is possible to change the direction of the reflected waves at will [2]. Developments in the field of antennas enabled creation of reflectarrays [3], layers with any desired phase of reflection at microwaves. Conceptually, reflectarrays are conventional mirrors, modified by some additional phase-shifting elements positioned close to fully reflecting surfaces. Since most reflectarrays incorporate a metal ground plane, the transmission through them is completely blocked and reflection amplitude can be very high if low-loss materials are used. On the other hand, the presence of a metal ground plane forbids transmission at all practically important frequencies and limits application possibilities. The use of metal meshes or frequency selective surfaces as back reflectors of reflectarrays does not allow one to overcome this drawback and implies, respectively, a very broadband reflection region or poor transmission above the resonant band [4]. If it will become possible to create arrays of small particles that fully reflect incident electromagnetic waves but allow full control over the reflection phase, all of the limitations due to the presence of a conventional mirror will be removed.

Clearly, such subwavelength structural layers possess electromagnetic properties that are not available in natural materials, and potential realizations require the use of artificial materials, called metamaterials. The past few years have witnessed remarkable progress in the development of single-layer planar metamaterials having deeply subwavelength thicknesses. Such two-dimensional composites, so-called metasurfaces [2,5], have demonstrated the capability to arbitrarily manipulate the reflected and transmitted wave fronts. While metasurfaces tailoring wave fronts in transmission [5–12] usually consist of subwavelength inclusions and are transparent outside of the operating frequency band, most metasurfaces manipulating reflection are metal backed and detectable over the entire frequency range [13–19]. To the best of our knowledge, the only work on phase-controlling reflecting structures without a ground plane utilizes a multilayer electrically thick structure [20]. The difficulties in extending the well-understood techniques for phase control in transmission to control of the reflection phase follow from the fact that the physical phenomena behind manipulation of wave fronts in transmission and reflection are crucially different. Transmission wave front control can be accomplished by using an array of various so-called Huygens elements (zero backward scattering inclusions) that scatter waves with adjustable phase in the forward direction [8–12]. To control the wave front of reflection, the inclusions in the array should be engineered in such a way that they re-radiate waves in the backward direction with different phases, while in the forward direction they scatter waves with the same phase, opposite to that of the incident plane wave.

In this Letter we introduce and experimentally validate a new concept of nonuniform metamirrors, ultrathin engineered structures providing full control of reflected wave

fronts independently for the two sides of the metamirror. Because of the lack of a ground plane and deeply subwavelength dimensions of the inclusions, the designed metamirrors are practically invisible at frequencies outside of the operational band. The proposed metamirrors are formed by single planar arrays of specifically shaped resonant bianisotropic inclusions [21,22] possessing both electric and magnetic responses, as well as magnetoelectric coupling.

Consider a metasurface consisting of a single planar periodic array of identical subwavelength inclusions polarizable both electrically and magnetically. An incident plane wave impinges on the array normally to its surface along the z direction (see Ref. [23]). Since the array period is small compared to the wavelength, the electric and magnetic moments induced in the inclusions can be modeled as surface-averaged electric and magnetic currents. The induced currents radiate secondary plane waves in the backward and forward directions. As shown in Ref. [21], it is convenient to describe the properties of a metasurface in terms of the collective polarizabilities α of its unit cell of the area S. The electric fields of the backward and forward scattered plane waves from the metasurface illuminated by an incident plane wave are given by

$$\mathbf{E}_{\text{back}} = -\frac{j\omega}{2S}(\alpha_e \pm 2\alpha_{\text{me}} - \alpha_m)\mathbf{E}_{\text{inc}},$$

$$\mathbf{E}_{\text{forw}} = -\frac{j\omega}{2S}(\alpha_e + \alpha_m)\mathbf{E}_{\text{inc}}, \qquad (1)$$

where ω is the angular frequency, α_e, α_m, and α_{me} are, respectively, the electric, magnetic, and so-called magneto-electric polarizabilities of the unit cell, normalized to the impedance of free space. The upper and lower signs in the equation correspond to the two different cases when the metamirror is illuminated from the $+z$ and $-z$ directions, respectively. The polarizability quantities characterize the electric and magnetic responses of the inclusions as well as their mutual interactions in the array. The magnetoelectric polarizability α_{me} measures the capability of the inclusion to acquire electric polarization under the influence of an external magnetic field. Such property, inherent in bianisotropic inclusions [22], enables additional freedom in metasurface engineering. Here we use the physical effect of bianisotropic coupling to allow realization of independent control of reflection and transmission using only small resonant particles. While all the particles are at resonance and create the same forward-scattered fields, different field coupling strength ensures the desired differences in reflection properties. This scenario allows realization of arbitrary (limited only by the power conservation) reflection and transmission properties of the structure.

It should be stressed here that the complete phase control of reflection can be achieved by exploiting an array of anisotropic particles with zero α_{me} and nonzero α_e and α_m

polarizabilities, such as simple electric and magnetic dipoles. However, the design of such an array becomes very challenging since the inclusions of these two types must operate in a metamirror at nonresonant frequencies [21] and be adjusted individually and very precisely, taking into account their mutual interactions.

Zero transmission through the metasurface is achieved when the inclusions collectively radiate a secondary wave in the forward direction that destructively interferes with the incident wave $\mathbf{E}_{\text{forw}} = -\mathbf{E}_{\text{inc}}$. To ensure full reflection with any desired phase ϕ, the backscattered wave must be such that $\mathbf{E}_{\text{back}} = e^{j\phi}\mathbf{E}_{\text{inc}}$. In order to efficiently manipulate wave fronts of reflection from metamirrors, we adjust the phase of reflection from each inclusion individually, preserving the unity value for the reflected-wave amplitude and identical phase (opposite to the phase of the incident wave) of the forward scattered fields. This feature dramatically distinguishes the metamirror concept from the designs utilizing a ground plane [13–17]. Figure 1 illustrates the effect of controllable asymmetric scattering. In this example, an array of inclusions radiates waves in the backward direction with a linearly varying phase.

To demonstrate the potential and flexibility of the proposed metamirror concept, we consider two example structures: a metamirror anomalously reflecting normally incident waves and a reflecting metalens (a single-layer focusing sheet). Although the proposed concept is generic and can be applied over the entire electromagnetic spectrum, we design and experimentally measure structures operating in the microwave frequency band. The designed
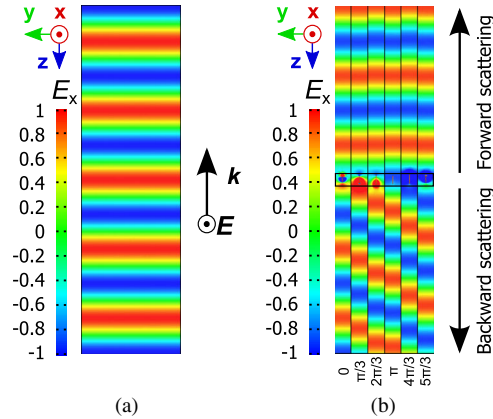

FIG. 1 (color online). The results of full-wave simulations of the individual inclusions of a metamirror which totally reflects normally incident waves at an angle $\theta = 45°$ from the normal. (a) Field distribution of an incident wave normally impinging on the metamirror surface. (b) Distribution of the copolarized electric field of the scattered waves from each inclusion. The forward scattered waves from the individual inclusions have identical phases opposite to the phase of the incident wave, which yields zero transmission. In the backward direction the inclusions radiate with discrete phase shifts from 0 to $5\pi/3$, clearly revealing anomalous reflection.

prototypes can be subsequently pushed to the infrared and even the optical range by downscaling the sizes of the structural inclusions, modifying their geometry, and taking into consideration the properties of materials at different frequencies. Recent progress in designing low-loss electromagnetic inclusions for the visible range [24] opens up a promising way to realize the proposed structures for light bending. In our design we are content with the case of metamirrors operating with incident waves of a single linear polarization. The polarization-insensitive regime in the metamirrors can be achieved by the use of inclusions possessing uniaxial symmetry [21].

First, we design a metamirror to efficiently reflect normally incident plane waves to an arbitrarily chosen angle $\theta = 45°$ from the normal. Based on the principle of phased arrays, the reflected wave front is deflected to an angle θ if the metasurface provides a linear phase variation spanning the 2π range with the periodicity $d = \lambda/\sin\theta$, where λ is the operating wavelength. In our design we use copper wire inclusions embedded in Rohacell-51HF ($\epsilon_r = 1.065$, $\tan\delta = 0.0008$) foam of 5 mm thickness [see Fig. 2(a)]. The dielectric substrate is needed only for mechanical support of small conductive inclusions. Each period d is discretized into 6 unit cells consisting of
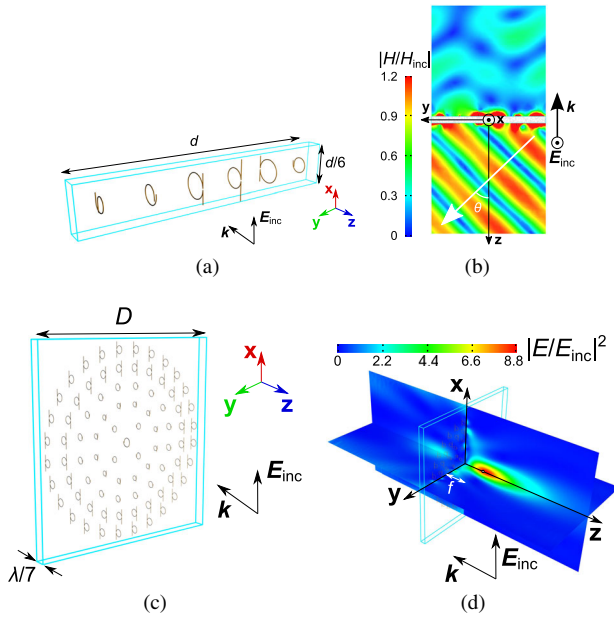

FIG. 2 (color online).   (a) The period of a metamirror consisting of 6 subwavelength copper inclusions that provide a linear phase variation of the reflection spanning a 2π range. The blue box denotes the dielectric substrate. (b) Magnetic field distribution (normalized to the magnetic field of the incident wave) of the transmitted (the $-z$ half-space) and the reflected (the $+z$ half-space) waves. (c) A metalens composed of 6 concentric arrays of the designed subwavelength inclusions. The dielectric substrate is denoted by the blue box. (d) Power density distribution (normalized to the incident power density) of the transmitted (the $-z$ half-space) and the reflected (the $+z$ half-space) waves.

different subwavelength inclusions providing discrete phase shifts from 0 to 2π (see Ref. [23]). All of the inclusions have nonzero magnetoelectric polarizability α_{me} due to the fact that they incorporate electrically polarizable straight wires connected to magnetically polarizable wire loops. The required polarizabilities α_e, α_m, and α_{me} of the inclusions were found based on Eq. (1). In order to determine the shape and dimensions of practically realizable inclusions with the required polarizabilities, we utilize an approach based on scattering cross sections [25]. All of the dimensions of the inclusions and a description of their electromagnetic polarizability can be found in Ref. [23].

The simulated scattering properties of the individual inclusions of the metamirror are shown in Fig. 1(b). The operating frequency of 5 GHz is chosen. At this frequency the periodicity along the y axis is $d = \lambda/\sin 45° = 84.9$ mm. Along the x axis the unit cells are positioned with the periodicity $d/6 = 14.1$ mm. An incident plane wave impinges on the metamirror from the $+z$ direction with the electric field parallel to the x axis. Figure 2(b) illustrates the simulated magnetic field distribution of the reflected (backward scattered wave) and transmitted waves (interference of the incident and forward scattered waves). Only 8% of the incident power is transmitted and 6% is absorbed by the material of the inclusions. The high reflectance of 86% and the pure wave front rotation confirm remarkable functionality of the metamirror. The reflection level can be further improved by optimizing the inclusions taking into account the mutual interaction of inclusions of different types. The half-power bandwidth of the proposed metamirror is 0.25 GHz or 5%, which can be considered quite broad taking into account the subwavelength thickness $t = \lambda/7$ of the designed structure. The frequency stability of the metamirror performance as well as its functionality for incident waves from the $-z$ direction are presented in Ref. [23]. It should be stressed that the proposed metamirror based on the wire inclusions is only a conceptual prototype and can be improved by using inclusions of other types [24,26,27] with the properties dictated by Eq. (1).

Another example demonstrating the universality of nonuniform metamirrors is focusing metasurfaces showing extremely strong wave-gathering ability. The metamirror concept opens a new route towards engineering a conceptually new kind of lens, one consisting of an ultimately thin single layer of subwavelength inclusions providing near-diffraction-limit focusing of electromagnetic energy at a chosen point. Subwavelength sizes of the inclusions that radiate as dipoles provide homogeneous phase variation along the surface and enable focusing at extremely short distances. We have designed a single-layer metalens composed of 6 concentric arrays of subwavelength inclusions with the dimensions described in Ref. [23] [see Fig. 2(c)]. The diameter of the lens is $D = 2.8\lambda$, and the effective thickness of the structure (thickness of the inclusions) is $t = \lambda/7$. The mechanically supporting

dielectric is a styrofoam plate ($\epsilon_r = 1.03$, $\tan\delta = 0.0001$) of 10 mm thickness. Realization of the desired lens response requires certain reflection phase variations along the surface ensuring that the scattered fields from all the inclusions constructively interfere at the desired point. Without loss of generality, we content ourselves with the case when the metalens confines energy on its axial line at a focal distance f. The required phase of reflection ϕ for an inclusion located at a distance r from the center is

$$\phi(r) = \phi_0 + \frac{\omega}{c}\sqrt{r^2 + f^2}, \qquad (2)$$

where c is the speed of light and ϕ_0 is an additional constant phase that can be chosen arbitrarily. Equation (2) shows that a metalens with a smaller focal distance requires faster phase variations along the surface. In order to have enough smooth phase gradient to allow surface homogenization, we choose the focal length of $f = 0.6\lambda$ for a metalens consisting of wire inclusions of $\lambda/7$ size. The relation between the phase ϕ and coordinate r of the inclusions of a metalens operating at 5 GHz is specified in Ref. [23].

An incident plane wave impinges on the metalens from the $+z$ direction with the electric field along the x axis. Figure 2(d) shows the simulated power distribution of the reflection and transmission from the metalens. The metalens effectively reflects the wave and focuses it tightly near the diffraction limit to a spot of only $2.8\lambda \times 0.9\lambda$ size ($1/e^2$ beamwidth). The extremely strong focusing ability of the designed metalens provides the focal length of only $f = 0.65\lambda$ and high energy gain of 8.8 in the spot. The unprecedentedly short focal length of our metalens is significantly smaller than those of conventional and other metamaterial-based lenses [7,8,28]. The f number (the ratio of the focal length to the aperture diameter of a lens f/D) for the designed metalens comes to 0.23 and can be further decreased by increasing the aperture, which in this example is only 2.8λ. Such a small f number of the metalens allows gathering more power and generally provides a brighter image. It should be noted that the metalens possesses asymmetrical focusing properties with respect to the propagation direction of incident waves (see Ref. [23]). An additional weak spot behind the metalens seen in Fig. 2(d) is caused by imperfections in the inclusions shape that affect the near-zone fields.

The operation of the two proposed metamirrors was verified by conducting measurements inside a parallel-plate waveguide. The measurement characterization is described in detail in Ref. [23]. The electric field distribution of the incident and reflected waves from the metamirror reflecting normally incident waves at an angle $\theta = 45°$ are shown in Figs. 3(a) and 3(b), respectively. The metalens operating in free space and described in Figs. 2(c) and 2(d) cannot be modeled in a waveguide due to the axial symmetry of the
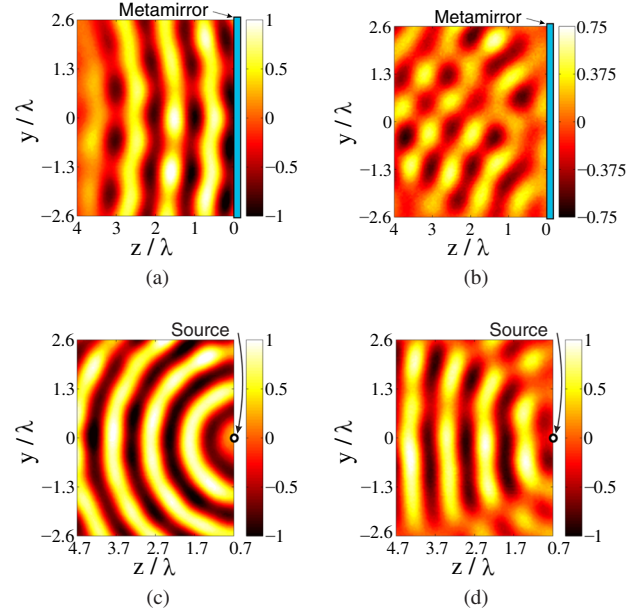

FIG. 3 (color online). Distribution of the measured (a) incident and (b) reflected copolarized electric field in the waveguide for a metamirror reflecting normally incident waves at an angle $\theta = 45°$. The source in (a) and (b) is located at point $z = 14\lambda$. Distribution of the measured (c) incident and (d) reflected copolarized electric field for a metalens in the waveguide. The metalens in (c) and (d) is positioned at point $z = 0$.

lens. Therefore, we manufacture a metalens with mirror symmetry along the xz plane focusing reflected waves in the line parallel to the x axis in the focal plane. To analyze the metalens, we position the source of an incident cylindrical wave in its focal plane (at a distance of $f = 0.65\lambda = 39$ mm). Based on the reciprocity principle, the metalens illuminated by an incident cylindrical wave from the focal point [shown in Fig. 3(c)] totally reflects a wave with a plane wave front [shown in Fig. 3(d)].

The above examples clearly demonstrate that arrays of small inclusions can fully reflect electromagnetic waves with any desired phase distribution. Control over the reflection amplitude can be realized simply by adjusting the loss parameter of the inclusions' material. Providing full control of reflected wave fronts, metamirrors are nearly transparent outside of the operational frequency band (see Ref. [23]). This unique feature leads to a variety of exciting applications over the entire electromagnetic spectrum. At microwaves, being practically transparent at infrared and visible frequencies, metamirrors have a clear potential for breakthroughs in the design of antennas for various applications, in particular, for satellites and radio astronomy. For example, the proposed layer can work as a large parabolic reflector for radio waves, while being deposited on a flat surface of a thin transparent film, dramatically simplifying deployment, or even on solar-cell panels of a satellite, not disturbing the panel operation. In radio astronomy as well as in satellite technologies, it will

*Corresponding author.
viktar.asadchy@aalto.fi

[1] J. M. Enoch, History of mirrors dating back 8000 years, Optom. Vis. Sci. **83**, 775 (2006).

[2] N. Yu and F. Capasso, Flat optics with designer metasur-faces, Nat. Mater. **13**, 139 (2014).

[3] D. M. Pozar, S. D. Targonski, and H. D. Syrigos, Design of millimeter wave microstrip reflectarrays, IEEE Trans. Antennas Propag. **45**, 287 (1997).

[4] N. Misran, R. Cahill, and V. F. Fusco, RCS reduction technique for reflectarray antennas, Electron. Lett. **39**, 1630 (2003).

[5] A. V. Kildishev, A. Boltasseva, and V. M. Shalaev, Planar photonics with metasurfaces, Science **339**, 1232009 (2013).

[6] N. Yu, P. Genevet, M. A. Kats, F. Aieta, J.-P. Tetienne, F. Capasso, and Z. Gaburro, Light propagation with phase discontinuities: Generalized laws of reflection and refrac-tion, Science **334**, 333 (2011).

[7] X. Ni, S. Ishii, A. V. Kildishev, and V. M. Shalaev, Ultra-thin, planar, Babinet-inverted plasmonic metalenses, Light Sci. Appl. **2**, e72 (2013).

[8] F. Monticone, N. M. Estakhri, and A. Alù, Full Control of Nanoscale Optical Transmission with a Composite Meta-screen, Phys. Rev. Lett. **110**, 203903 (2013).

[9] C. Pfeiffer and A. Grbic, Metamaterial Huygens' Surfaces: Tailoring Wave Fronts with Reflectionless Sheets, Phys. Rev. Lett. **110**, 197401 (2013).

[10] C. Pfeiffer, N. K. Emani, A. M. Shaltout, A. Boltasseva, V. M. Shalaev, and A. Grbic, Efficient light bending with isotropic metamaterial Huygens' surfaces, Nano Lett. **14**, 2491 (2014).

[11] F. Wang, Q.-H. Wei, and H. Htoon, Generation of steep phase anisotropy with zero-backscattering by arrays of coupled dielectric nano-resonators, Appl. Phys. Lett. **105**, 121112 (2014).

[12] C. Pfeiffer and A. Grbic, Controlling Vector Bessel Beams with Metasurfaces, Phys. Rev. Applied **2**, 044012 (2014).

[13] S. Sun, K.-Y. Yang, C.-M. Wang, T.-K. Juan, W. T. Chen, C. Y. Liao, Q. He, S. Xiao, W.-T. Kung, G.-Y. Guo, L. Zhou, and D. P. Tsai, High-efficiency broadband anomalous reflection by gradient meta-surfaces, Nano Lett. **12**, 6223 (2012).

[14] A. Pors, M. G. Nielsen, R. L. Eriksen, and S. I. Bozhevolnyi, Broadband focusing flat mirrors based on plasmonic gradient metasurfaces, Nano Lett. **13**, 829 (2013).

[15] A. Pors and S. I. Bozhevolnyi, Plasmonic metasurfaces for efficient phase control in reflection, Opt. Express **21**, 27438 (2013).

[16] M. Farmahini-Farahani and H. Mosallaei, Birefringent reflectarray metasurface for beam engineering in infrared, Opt. Lett. **38**, 462 (2013).

[17] M. Esfandyarpour, E. C. Garnett, Y. Cui, M. D. McGehee, and M. L. Brongersma, Metamaterial mirrors in optoelec-tronic devices, Nat. Nanotechnol. **9**, 542 (2014).

[18] M. Kim, A. M. H. Wong, and G. V. Eleftheriades, Optical Huygens' Metasurfaces with Independent Control of the Magnitude and Phase of the Local Reflection Coefficients, Phys. Rev. X **4**, 041042 (2014).

[19] M. Veysi, C. Guclu, O. Boyraz, and F. Capolino, Thin anisotropic metasurfaces for simultaneous light focusing and polarization manipulation, J. Opt. Soc. Am. B **32**, 318 (2015).

[20] C. Saeidia and D. Weide, Wideband plasmonic focusing metasurfaces, Appl. Phys. Lett. **105**, 053107 (2014).

[21] Y. Radi, V. S. Asadchy, and S. A. Tretyakov, Tailoring reflections from thin composite metamirrors, IEEE Trans. Antennas Propag. **62**, 3749 (2014).

[22] A. N. Serdyukov, I. V. Semchenko, S. A. Tretyakov, and A. Sihvola, *Electromagnetics of Bi-anisotropic Materials: Theory and Applications* (Gordon and Breach Science, Amsterdam, 2001).

[23] See Supplemental Material at http://link.aps.org/supplemental/10.1103/PhysRevLett.114.095503 for addi-tional information on the design and measurement charac-terization of the proposed metamirrors.

[24] S. Campione, L. I. Basilio, L. K. Warne, and M. B. Sinclair, Tailoring dielectric resonator geometries for directional scattering and Huygens' metasurfaces, Opt. Express **23**, 2293 (2015).

[25] V. S. Asadchy, I. A. Faniayeu, Y. Radi, and S. A. Tretyakov, Determining polarizability tensors for an arbitrary small electromagnetic scatterer, Photon. Nanostr. Fundam. Appl. **12**, 298 (2014).

[26] G. R. Keiser, A. C. Strikwerda, K. Fan, V. Young, X. Zhang, and R. D. Averitt, Decoupling crossover in asymmetric broadside coupled split-ring resonators at terahertz frequen-cies, Phys. Rev. B **88**, 024101 (2013).

[27] Y. Cheng, H. Yang, Z. Cheng, and B. Xiao, A planar polarization-insensitive metamaterial absorber, Photon. Nanostr. Fundam. Appl. **9**, 8 (2011).

[28] J. Neu, B. Krolla, O. Paul, B. Reinhard, R. Beigang, and M. Rahm, Metamaterial-based gradient index lens with strong focusing in the THz frequency range, Opt. Express **18**, 27748 (2010).